

Compound Dihuang Granule Changes Gut Microbiota of MPTP-Induced Parkinson's Disease Mice via Inhibiting TLR4/NF- κ B Signaling

Zhu-qing He

Shanghai Municipal Hospital of Traditional Chinese Medicine, Shanghai University of Traditional Chinese Medicine

Peng-fei Huan

Shanghai University of Traditional Chinese Medicine

Li Wang (✉ zyzd8434@shutcm.edu.cn)

Shanghai University of Traditional Chinese Medicine

Jian-cheng He

Shanghai University of Traditional Chinese Medicine

Research Article

Keywords: Parkinson's disease, compound Dihuang Granule, Gut microbiota, Neuroinflammation, TLR4/NF- κ B pathway, network pharmacology

Posted Date: November 28th, 2022

DOI: <https://doi.org/10.21203/rs.3.rs-2300112/v1>

License: © ⓘ This work is licensed under a Creative Commons Attribution 4.0 International License. [Read Full License](#)

Additional Declarations: No competing interests reported.

Version of Record: A version of this preprint was published at Neurochemical Research on August 10th, 2023. See the published version at <https://doi.org/10.1007/s11064-023-04004-9>.

Abstract

Intestinal flora was connected to Parkinson's Disease (PD) pathology. The ancient Chinese medication for PD is Compound Dihuang Granule (CDG), and we found a neuroprotective function in treating the constipation of PD patients. Nevertheless, the mechanism of action still needs to be clarified. We predicted the probable targets of CDG against PD through Traditional Chinese medicine (TCM) network pharmacology and verified the analysis through animal experiments *in vivo*. The protein-protein interaction (PPI) network analysis screened PD-related genes, including TLR4, TBK1, NF- κ B (NF- κ B p65), and TNF(TNF- α). Gene Ontology (GO) and Kyoto Encyclopedia of Genes and Genomes (KEGG) analyses proved that the NF- κ B and toll-like receptor signaling pathways serve a key function in CDG therapy of PD. Molecular docking analysis demonstrated that CDG strongly connected to TLR4/NF- κ B. Experiments findings indicated that CDG improved the damage of DA neurons and gut microbial dysbiosis, ameliorated motor impairments, and suppressed the PD-associated inflammation and oxidative stress in mice induced by MPTP. CDG suppressed the inflammatory proteins in the colon and protected the intestinal barrier. Overall, CDG improved gut microbial in PD by blocking the pathway of TLR4/NF- κ B.

Introduction

Parkinson's disease (PD) is connected to extremely high morbidity and mortality [1]. PD pathogenesis is the outcome of interacting genetic and environmental variables, and its typical pathological features are DA neurons selective degradation in the substantia nigra (SN) and Lewy body creation [2, 3]. Non-motor symptoms (NMS) of PD patients are PD prodromal manifestations, such as gastrointestinal dysfunction (dysphagia, gastric emptying delay, and constipation) that predate motor signs (static tremor, stiffness, and bradykinesia) [4, 5]. Besides being among the most prevalent non-motor signs in PD patients, constipation is a recognized feature of prodrome PD, which has a hugely adverse consequence on the survival and living standard of PD patients, hypothesizing that PD arises in the intestine [4, 6, 7].

Recently, many researchers demonstrated that intestinal flora is associated with PD pathology. With modern science and technologies, including 16S rDNA sequencing, and metabolomics, intestinal microbiota and brain-gut could transmit information in two directions, the "microbe-gut-brain axis" [8, 9]. Moreover, intestinal bacteria affect neural development and participate in brain function and body metabolism, and entheogenic encephalopathy serves a crucial role in neurodegenerative diseases [10]. Toll-like receptor-4 (TLR4) did a vital part in recognizing microbial components, activating NF- κ B signaling, and releasing the inflammatory cytokine Interleukin-1 β (IL-1 β), tumor necrosis factor- α (TNF- α), Interleukin-6 (IL-6) [11, 12].

Moreover, constipation in PD patients is connected with intestinal bacterial dysbiosis and -synuclein aggregates in the enteric nervous system [13, 14]. Studies have shown gut microbiota variations between healthy controls and PD patients [15]. Bacteroides abundance decreased, exercised symptoms and constipation symptoms improved significantly in PD patients after fecal microbiota transplantation (FMT) [16]. Although the dysbiotic gut microbiota has a function in PD disease pathogenesis, the concrete mechanism is obscure.

Compound Dihuang Granule (CDG) is a traditional Chinese medicine used for treating PD. It exerted a significant neuroprotective effect through multiple targets and could effectively improve gastrointestinal dysfunction in PD rats [17, 18]. Our previous study found that CDG decreased inflammatory factor expression NF- κ B and inflammatory cytokines IL-6 and TNF- α in PD mice [19]. However, CDG particular mechanism of action remains obscure.

Network pharmacology is a frontier discipline that uses various omics and network analysis technologies to build and reveal the connection among drugs, components, targets, and diseases, elaborate the mechanism of drug action, and explore the correlation between drugs and diseases. This method is often used to analyze the action mechanism of multi-target medicines in complex conditions [20]. We used Cytoscape software to build a "herb-component-target-pathway" network and made molecular docking with the core active components of CDG and the core action targets. CDG might treat PD by TLR4/NF- κ B signal pathway. Therefore, we focused on TLR4/NF- κ B signal pathway and sought to analyze the neuroprotective role of CDG in regulating intestinal flora imbalance by treating mice with MPTP-induced PD and exploring its practical mechanism.

Methods

CDG Preparation

CDG is effective for treating PD and is composed of seven traditional Chinese medicines: Shú dì huáng (*Rehmannia glutinosa* (Gaertn.) DC.), Bái sháo (*Paeonia lactiflora* Pall), Gōu tēng (*Uncaria rhynchophylla* (Miq.) Miq. ex Havil), Zhēn zhū mǔ (*Hyriopsis cumingii* (Lea)), Dān shēn (*Salvia miltiorrhiza* Bge), Shí chāng pú (*Acorus tatarinowii* Schott), Quán xiē (*Buthus martensii* Karsch). Herein, the English name of herbal medicines referred to the Chinese pharmacopeia, and the CDG standard utilized followed the Chinese pharmacopeia (2010 version). The CDG was prepared and subjected to quality control analysis using LC-MS spectrometry [17].

Network pharmacology analysis

Screening and predicting the target of active components of CDG

The active ingredients of CDG were obtained from (<http://bionet.ncpsb.org/batman-tcm/> and <http://tcmispw.com/databases>). Active ingredients of CDG were selected satisfying that a drug-likeness (DL) ≥ 0.18 or score cutoff ≥ 20 in addition to an oral bioavailability (OB) $\geq 30\%$. PD-related targets were taken from the Therapeutic Target Database (TTD; <http://db.idrblab.net/ttd/>), Online Mendelian Inheritance in Man (OMIM, <https://omim.org/>), Genecards (<https://www.genecards.org/>), PharmGBK (<https://www.pharmgkb.org/>), and DrugBank (<https://go.drugbank.com/>), Comparative Toxicogenomics Database (CTD; <http://ctdbase.org/>), DisGeNET (<https://www.disgenet.org/>).

Target PPI Network Construction

We matched the obtained CDG active components with PD-related targets, and the intersection target was considered the target of CDG treatment of PD, which was presented with a Venn diagram. Then, the shared goals of CDG and PD were loaded into STRING (<https://string-db.org/>), and Cytoscape (3.8.0) was used to build a protein-protein interaction (PPI) network. Meanwhile, the median values greater than EC, DC, CC, BC, LAC, and NC were utilized as screening factors to identify the possible core target of CDG in treating PD.

Gene Ontology (GO) and Kyoto Encyclopedia of Genes and Genomes (KEGG) analyses

To investigate the biological processes and mechanisms implicated in PD treatment by CDG, GO and KEGG enrichment analyses were done for candidate targets. Therefore, the finding showed that GO terms or KEGG pathways having a P -value < 0.05 were regarded to be significant.

Molecular docking

The essential active ingredients of CDG were selected for molecular docking with the core target. PyMOL (2.4.0) Software was utilized to eliminate water molecules and ligands from core target proteins. AutoDock Vina software was employed to dock the receptor protein with the small ligand molecule and finally obtain its conformation.

Experimental Validation

Animals and experimental design

Male C57BL/6 mice that were 7–8 weeks old and weighed 20 ± 2 g were acquired from Shanghai Slake Experimental Animal Co. Ltd. (Shanghai, China). Mice were fed and drank water ad libitum and kept in standard environments (at $22 \pm 2^\circ\text{C}$, humidity $55 \pm 10\%$, 12 h light/dark cycle) in compliance with the permission of the Experimental Animal Ethics Committee of Shanghai University of Chinese Medicine (PZSHUTCM200717037).

In total, 24 C57BL/6 mice were haphazardly split into the control group (Normal), the model group (MPTP), as well as the treatment group (CDG; each $n = 8$). The model and treatment groups received 1-methyl-4-phenyl-1,2,3,6-tetrahydropyridine (MPTP, 30 mg/kg) by intraperitoneal (i.p.) injection to construct the PD model, and the normal mice were given equal normal saline. Each group received an injection once a day for five successive days. After molding, 10 g/kg CDG was given to mice in the treated group, while the other two groups were given normal saline for seven days. Behavioral training was given for three days before behavioral testing, and after the treatment, all groups of mice underwent behavioral testing, and fresh feces and tissues were collected. Figure 1 represents the experimental flow chart.

Behavioral experiments

An open field test was conducted in 30 cm × 30 cm absenteeism. Prior to the experiment, the mice habituated to their surroundings for 1 h. The mice were then set in the field center, and the camera recorded the mice for 5 min. After the experiment, real-time video recording analyzed the distance from the center point and the residence time.

The Pole test was done by placing the ball head on the pole and training mice to revolve and go up the pole. The turn time and climbing time of each group were recorded. All mice were tested three times and averaged as the final result.

Collecting samples and preparing tissue

The mice from each group were individually placed in an empty, clean high-pressure cage, and the feces were instantly gathered in sterile EP tubes and kept at -80°C . Tissues from the brain, colon, and serum were recovered for the study.

Western blot analysis

RIPA buffer (Beyotime, Shanghai, China) was used with 1% phenylmethanesulfonyl fluoride (PMSF) (Beyotime, Shanghai, China) to isolate the total protein. Therefore, the homogenized protein was centrifuged at 13,000 rpm, 4°C for 5 min to recover the total protein, and mixed with SDS loading buffer to boil for 10 min for denaturation. Total protein levels were evaluated with a BCA kit (Takara, Shanghai, China). A 30 μg of total protein was isolated using 10% sodium dodecyl sulfate-polyacrylamide gel electrophoresis (SDS-PAGE), transmitted to polyvinylidene difluoride (PVDF) membranes, then incubated at 4°C overnight of the subsequent antibodies: Tyrosine hydroxylase (1:1000; 58844, Cell Signaling Technology), TBK1 (1:1000; abs132000, Absin), NF- κB p65 (1:1000; 8242S, Cell Signaling Technology), TNF- α (1:1000; 11948, Cell Signaling Technology), TLR4 (1:1000; abs132000, Absin), Beta Actin (1:2000; 20536-1-AP, Proteintech). Therefore, incubated with secondary antibodies anti-rabbit IgG(1:10000; 5151S, Cell Signaling Technology) or Anti-mouse IgG (1:10000; 5470S, Cell Signaling Technology) for 1 h. The blots were discovered utilizing the LI-COR Odyssey system (Odyssey CLx, USA), and ImageJ analyzed the densities.

Immunohistochemistry (IHC)

Brain tissues were dehydrated at 20% sucrose. After tissue sinking, the 30% sucrose solution was dehydrated and sectioned. Brain tissue was cut into 30 μm thickness and selected from SN was blocked in 10% BSA 37°C for 1 h after that incubated with anti-tyrosine hydroxylase (1:1000, sc-25269 AC, Sigma). Then, ABC universal mini-plus kit (ZG0615, VECTOR) was utilized. Positive cells number were measured using ImageJ.

Immunofluorescence (IF) staining

The tissue of the brain and colon at 30 μm thickness was frozen. Then, sections were incubated with 0.3% BSA in 5% Triton X-100 at room temperature (RT) for 1 h. Sections were incubated at 4°C overnight with primary antibodies: tyrosine hydroxylase (1:500; sc-25269 AC, Sigma), TNF- α (1:1000; 11948, Cell Signaling Technology), TLR4 (1:1000; abs132000, Absin), GFAP (1:1000; 80788S, Cell Signaling Technology), Iba-1 (1:400; 019-19741, Wako), ZO-1 (ab96587; Abcam), then incubated with secondary antibodies anti-rabbit IgG (1:1000; 4412, Cell Signaling Technology) or Anti-mouse IgG (1:1000; 4409S, Cell Signaling Technology) for 1h at 37°C . A confocal microscope was used to observe the images, and Image J was used to calculate positive cells.

Enzyme-linked immunosorbent assay (ELISA)

Shanghai Weiao Biotechnology Company offered the ELISA kit to examine the expression of superoxide dismutase (SOD), malondialdehyde (MDA), interleukin-1 β (IL-1 β), and tumor necrosis factor-alpha (TNF- α) in the mice serum. The experimental methods were conducted.

16S rDNA microbiota profiling

Utilizing CTAB DNA was isolated from many mice fecal samples. 16S rDNA sequencing was done on the NovaSeq PE250 platform (Illumina, San Diego, CA, USA). The V3-V4 regions on bacterial 16S rDNA genes were amplified with forward (F341F5'-CCTACGGGNGGCWGCAG-3') and reverse (805R 5'-GACTACHVGGGTATCTAATCC-3') primers [21]. We conducted first denaturation at 98°C for 30 s; 32 cycles of denaturation at 98°C for 10 s, annealing at 54°C for 30 s, and extension at 72°C for 45 s; and a final extension at 72°C for 10 min as PCR conditions amplify prokaryotic 16S fragments. Experiments, including DNA extraction and detection, PCR amplification, product purification, library construction, and high-throughput sequencing, were done utilizing Lc-Bio technologies (Hangzhou, China).

Bioinformatics analysis

Three parameters (Chao1, Shannon, and Simpson) were used in the QIIME program. The species diversity complexity Each sample was analyzed using alpha diversity. QIIME2 estimated beta diversity. We used the SILVA (Release 132; <https://www.arb-silva.de/documentation/release-132/>) and the NT-16S database for the classification of species in addition to subsequent evaluation to confirm the accomplishment and accuracy of the annotation results. Utilizing R (v3.5.2), a principle coordinates analysis (PCoA), heatmap analysis, Bray-Curtis similarity clustering, as well as species abundance analysis, were conducted.

Statistical analysis

GraphPad Prism8 software reported experimental data as mean \pm standard deviation (SD). Findings were measured utilizing one-way analysis of variance (ANOVA) or non-parametric Kruskal-Wallis test, with a $P < 0.05$ showing a significant difference.

Results

Network pharmacology research

Screening targets and active ingredients of CDG

Herein, active ingredients from CDG were finally screened from the related database, and 285 targets were obtained after removing and merging (Fig. 1A, File S1). Moreover, 1874 disease targets were obtained from the databases of Drangbank, PharmGKB, GeneCard CTD, OMIM, DisGeNET, and NCBI (Fig. 1A, File S2). The Venn diagram shows the obtained 150 CDG and PD intersection targets (Fig. 1A, File S3).

PPI network analysis of CDG treatment for PD

To explore the interaction between 150 common targets, we imported them into the STRING data analysis network to build a PPI network and visualized on Cytoscape (Fig. 1A). We finally obtained 21 core targets that played an important role in PD, including TLR4, TBK1, NF-KB, and TNF (Fig. 1B, File S4).

GO and KEGG enrichment analyses

Based on p -value screening, we selected the top 30 items of GO and KEGG analyses based on the P -value (Fig. 1C, File S5). According to the screening results, BP mainly involved the response to the nutrient level and cellular response to lipids. CC Analysis found that it mainly included an integral component of the presynaptic membrane, vessel lumen, and inflammation. MF analysis demonstrated that the targets were primarily included in the transcription factor binding and alpha-adrenergic receptor activity. CDG might exert therapeutic PD by participating in multiple biological processes. Through KEGG enrichment analysis, the pathways involving core targets were obtained, including the NF- κ B and Toll-like receptor signal pathways (Fig. 1C, File S6). Moreover, the findings also demonstrated that the target genes of CDG active components were strongly connected to PD and linked to other diseases, including tumors, lipids, atherosclerosis, and infectious diseases, suggesting the potential advantages of CDG in treating these diseases.

Molecular docking

Figure 2 illustrates findings of molecular docking; the screened active components 1,2,5,6-tetrahydroptanshinone, Beta-sitosterol, and Kaempferol had good binding energy with TLR4 (Binding energy: -7.04 KJ \cdot mol $^{-1}$, -6.39 KJ \cdot mol $^{-1}$, -5.58 KJ \cdot mol $^{-1}$; Figs. 2A-C). Quercetin had a good combining ability with NF-KB and TBK1 (Binding energy: -6.24 KJ \cdot mol $^{-1}$, -6.31 KJ \cdot mol $^{-1}$, Figs. 2D-E). Moreover, kaempferol had a good binding ability to TNF- α (Binding energy: -6.95KJ \cdot mol $^{-1}$, Fig. 2F).

Experimental validation

CDG improved motor functions in MPTP-induced PD mice by avoiding dopaminergic neuronal death

Motor disorders and DA neuron injury are commonly present in PD models. Open field and pole tests were performed on animals to evaluate the possible neuroprotective effect of CDG on the motor function of MPTP-induced mice. Open field test demonstrated that motor dysfunction in the MPTP group was reflected in the reduced total motor distance and increased dwell duration in the central area ($P < 0.001$, $P < 0.001$, MPTP vs. Normal; Figs. 3A-C). CDG significantly improved the exercise ability and exploration ability of the PD mice ($P < 0.001$, $P < 0.001$, CDG vs. MPTP; Figs. 3B-C). Pole test results found that

PD mice exhibited a significantly reduced capacity for grip ability, showing a significantly longer head-turning time and pole climbing time ($P < 0.001$, $P < 0.001$, vs. Normal), and CDG treatment improved motor function of MPTP-induced PD mice ($P < 0.001$, $P < 0.001$, vs. MPTP; **Fig. 3D-E**).

Moreover, we further examined alterations of dopaminergic neurons in SN, and TH expression, which is a dopaminergic biomarker. Immunohistochemical staining findings noted that the shape of TH-positive cells became blurred, and TH-positive cells expression was also decreased significantly when contrasted with the normal group mice ($P < 0.001$), and the TH expression was significantly raised after CDG treatment ($P < 0.01$, **Figs. 3F-G**). Meanwhile, Western blot (WB) analysis with anti-TH antibody validated the above results ($P < 0.01$, vs. Normal; $P < 0.01$, vs. MPTP; **Figs. 3H-I**).

CDG improves the Gut microbial dysbiosis of MPTP-induced PD mice

We observed the species abundance, evenness, and intestinal microbiota distribution among the mice, including alpha and beta diversity analysis by 16S rDNA sequencing. Figure 4A depicts non-significant differences between the three groups by the alpha diversity indices (Chao1, **File S7**). The results showed the microbial composition difference between the three groups (**Fig. 4B, File S8**). We analyzed the species composition and differences in the samples to further identify the potential bacterial groups of microbial dysbiosis. We presented the abundance and composition of each group using a heatmap (**Figs. 4D and F, File S9**). At the phylum level, the dominating bacteria were Bacteroides, Firmicutes, and Proteobacteria (**Fig. 4C**). We found a significant increase in the predominance of Proteobacteria, Patescibacteria in the MPTP group ($P < 0.01$, $P < 0.01$ vs. Normal), and reduced after CDG administration ($P < 0.01$, vs. MPTP; **Table. 1**). At the genus level, the dominating bacteria mainly included Muribaculaceae_unclassified, Lactobacillus, and Ruminococcaceae_UCG-014 (**Fig. 4E**). PD mice showed decreased Lactobacillus, Bilophila, Candidatus_Saccharimonas, and Ruminococcaceae_UCG-005 at the genus level ($P < 0.05$, $P < 0.01$, $P < 0.05$, $P < 0.05$, vs. Normal), and increased Lactobacillus, Ruminococcaceae_UCG-014, Candidatus_Saccharimonas, Enterorhabdus after CDG therapy ($P < 0.05$, $P < 0.01$, $P < 0.01$, $P < 0.05$, vs. MPTP; **Table. 1**). Meanwhile, the predominance of Muribaculum, Turicibacter, Desulfovibrio were raised at genus in PD mice ($P < 0.01$, $P < 0.05$, $P < 0.01$, vs. Normal). CDG mice showed a lowered predominance of Muribaculum and Turicibacter ($P < 0.001$, $P < 0.05$, vs. MPTP; **Table. 1**).

CDG ameliorated neuroinflammation and oxidative stress in MPTP-induced PD mice

Given that gut dysbiosis could promote inflammation as well as oxidative stress in the brain of PD patients and trigger the excessive response of the immune system accompanied by systemic inflammation [11]. Glial activation is strongly associated with PD neuroinflammation development [22, 23]. We observed the expression of GFAP and Iba1 (green) with TH (Red) colocalization in SN neurons utilizing immunohistochemistry staining. The findings demonstrated that GFAP and Iba1 expressions showed significant upregulation after MPTP injury in model group mice ($P < 0.001$, $P < 0.001$, vs. Normal, **Figs. 5A-D**), and we found a significant decrease in GFAP and Iba1 expressions after CDG therapy than the model group ($P < 0.001$, $P < 0.001$, vs. Normal, **Fig. 5A-D**). Concurrently, the morphological changes in GFAP⁺ and Iba1⁺ cells were found. The data above demonstrated that CDG reduced both GFAP and Iba1 increase and ameliorated the neuroinflammation in MPTP-induced PD mice.

Utilizing ELISA, the experimental findings demonstrated that inflammatory factor IL-1 β and TNF- α expressions were lowered significantly after CDG treatment ($P < 0.05$, $P < 0.05$, vs. MPTP; **Figs. 5E-F**). We also assayed two related genes expression associated with oxidative stress, SOD and MDA. We observed a significant rise in MDA level and decrease in SOD activity in PD mice ($P < 0.01$, $P < 0.001$, vs. Normal), CDG treatment lowered MDA level and raised SOD activity ($P < 0.05$, $P < 0.001$, vs. MPTP; **Fig. 5G-H**). The above experimental findings proved that CDG ameliorated the neuroinflammation and oxidative stress in MPTP-induced PD mice.

CDG suppresses colonic inflammation and intestinal leakage in MPTP-induced PD mice

Usually, gut dysbiosis may result in intestinal permeability and activate TLR signaling. We further examined whether CDG modulated gut integrity and examined the expression of the key mediator TLR4 and inflammatory factor TNF- α in colonic tissue. IF assay showed that TLR4 and TNF- α cells expression increased in PD mice colon ($P < 0.001$, $P < 0.001$, vs. Normal) and significantly decreased after CDG therapy ($P < 0.001$, $P < 0.01$, vs. MPTP; **Figs. 6A-B and D-E**). Gut barrier integrity is directly associated with tight junction protein expression (ZO-1) in intestinal tissue [24]. ZO-1 cells were continuously expressed in the colon of normal mice, and the intestinal mucosal integrity of PD mice was destroyed, and ZO-1 expression significantly lowered ($P < 0.001$, vs. Normal), its expression raised significantly after CDG therapy ($P < 0.001$, vs. MPTP; **Figs. 6C and F**).

CDG regulated gut flora and ameliorated neuroinflammation via inhibiting TLR4/NF- κ B pathway in MPTP-induced PD mice

To determine if TLR4 / NF- κ B signaling was a potential target of CDG in regulating gut flora and ameliorating neuroinflammation, we evaluated the TLR4 / NF- κ B signaling expression-associated proteins in colonic and striatum tissue using WB. Findings revealed that TLR4 expression, TBK1, NF- κ B p65, and TNF- α proteins increased significantly in the striatum of PD mice ($P < 0.001$, $P < 0.001$, $P < 0.001$, $P < 0.001$, vs. Normal), and the above indices were all significantly decreased with CDG therapy ($P < 0.05$, $P < 0.05$, $P < 0.001$, $P < 0.001$, vs. MPTP; **Figs. 7A and 7C-F**). In parallel, TLR4, TBK1, NF- κ B p65, and TNF- α protein expressions were significantly raised in PD mice colon ($P < 0.001$, $P < 0.001$, $P < 0.001$, $P < 0.001$, vs. Normal); and TLR4, TBK1, NF- κ B p65, and TNF- α expression exhibited a significant reduction in the colon after CDG treatment ($P < 0.001$, $P < 0.001$, $P < 0.001$, $P < 0.001$, vs. MPTP; **Figs. 7B and 7G-J**) The above results indicated that CDG might regulate gut flora and reduce the inflammation level by reducing the pathway of TLR4/NF- κ B.

Discussion

Currently, there are no truly ideal methods for optimal targeted drug treatments for PD. It has become a research hotspot for decreasing toxicity and side effects of anti-PD medications and finding alternative drugs. TCM typically showed a multi-component and multi-pathway synergistic effect in treating PD. Compound Dihuang Granule was developed associated with clinical experience in treating PD. To further study the CDG mechanism in treating PD, we screened the key active components of CDG in treating PD utilizing network pharmacology and found that the CDG mechanism in treating PD could be closely

associated with the Toll-like receptor and NF-KB pathways. Therefore, the following animal experiments will verify essential proteins expression on TLR4/NF-KB signal pathway and further explore the potential molecular pathway of CDG treatment of PD.

Our previous study demonstrated that CDG played a significant neuroprotective role in the MPTP-induced PD model and the 6-OHDA-induced PD model in vivo and could effectively improve gastrointestinal dysfunction and suppress microglia activation in PD mice [17, 18, 25]. Gut microbiosis is a potential factor in PD pathogenesis, and that gut microbiota was connected to PD progression by the gut-brain axis interaction [26, 27]. Herein, intraperitoneal MPTP injection was used to establish a PD mouse model related to intestinal microbiota disorders to measure CDG neuroprotective effect on PD and further study its treatment mechanism.

PD research has thoroughly studied MPTP, among the highest-known neurotoxins disrupting dopaminergic neurons [28]. Due to its lipophilicity, MPTP might pass the blood-brain barrier, transforming it to MPDP⁺ by monoamine oxidase B in astrocytes. MPP⁺ is the active compound of dopamine neurons that enters the SNpc. It suppresses complex I of the mitochondrial electron transport chain, resulting in reduced ATP, oxidative stress, as well as degeneration of DA ergic neurons [29, 30, 31]. Herein, MPTP-induced PD mice exhibited motor dysfunctions in open-field and pole tests. Oxidative stress was crucial in PD development and might induce degeneration of DA ergic neurons. SOD, a radical scavenger, and MDA, a lipid peroxidation metabolite, are important indicators revealing oxidative stress levels [32, 33].

Moreover, PD mice had increased MDA and decreased SOD expression in serum, which had an oxidative stress response. IHC of brain tissue and WB showed DA damage. Together, MPTP-induced mice had PD pathology and motor symptoms. Furthermore, MPTP-induced PD mice exhibited dysbiota dysbiosis [34, 35, 36]. Therefore, we analyzed the composition of the gut microbiota in PD mice by 16s rDNA sequencing. The findings demonstrated a non-significant variation in alpha diversity among the three groups, indicating that our sample sizes should be increased. Alpha diversity showed no changes between PD patients and principal normal subjects [37]. Moreover, beta diversity changed significantly among the three groups. Proteobacteria and Patescibacteria abundance increased significantly in PD mice at the phylum level. Proteobacteria were associated with gastrointestinal inflammation, with higher content in PD patients, and increased Proteobacteria abundance in PD mice with MPTP molding [34, 38], consistent with our animal experiments. Lactobacillus is a probiotic bacterium that is reduced in PD patients and has also been reduced in MPTP-induced mice [5, 39].

Additionally, we first found that Genus Muribaculum and Candidatus_Saccharimonas were associated with the PD, with increased Muribaculum and decreased Candidatus_Saccharimonas in MPTP-induced PD mice. As per our results, the decreased Genus Bilophila abundance was associated with PD. Bilophila abundance is correlated with Hoehn and Yahr stages, revealing that Bilophila can serve as a progression indicator in PD [40]. Desulfovibrio can produce hydrogen sulfide and LPS, which may induce the aggregation of α -synaptic nuclear proteins, with a higher abundance as observed in PD patients [41], also increased at Genus herein. Briefly, MPTP-induced mice had dysbiota dysbiosis, and the mechanisms of intestinal microbiota in PD progression still need further exploration.

Further analysis of the microbiota revealed that reestablishing normal gut microflora could enable the protective effect of CDG therapy. CDG increased the abundance of Phylum Firmicutes in PD mice. Firmicutes can produce butyrate, which is involved in the inflammatory response of body [42]. SCFAs have crucial roles in promoting intestinal function and anti-inflammatory effects. Ruminococcaceae_UCG-005 and Ruminococcaceae_UCG-014 can produce SCFAs and exert their anti-inflammatory effects [43, 44]. Herein, Genus Ruminococcaceae_UCG-005 was reduced in PD mice, and Genus Ruminococcaceae_UCG-014 was increased after CDG treatment, adjusting for the microflora of PD mice. Moreover, the abundance of beneficial bacteria Enterorhabdus was increased after CDG administration. Turicibacter is associated with disordered lipid metabolism and can exert anti-inflammatory effects, and Turicibacter is positively associated with SCFA production [45]. Herein, the predominance of Turicibacter was raised in the PD mice after CDG administration. The increase of Turicibacter in the model group might be associated with the PD immunomodulation of mice. Overall, our data supported that CDG significantly altered some inflammation-associated microflora in MPTP-induced mice, increasing beneficial bacteria.

Gut microbiota and its metabolites can participate in PD pathophysiology by regulating CNS neuroinflammation, gut inflammation, and barrier function through gut-brain axis interactions [46]. Dysbiosis of gut microbes might cause bacteria to produce harmful metabolites, such as lipopolysaccharides (LPS), which could disrupt the functionality of gastrointestinal barrier. TLR4 is the primary receptor for LPS immune recognition, widespread express on the surface of several cells, including microglial, astrocyte, and intestinal epithelial cells. Its activation triggers the host inflammatory response and the proinflammatory factors, including TNF- α , IL-1 β , and IL-6 [47, 48, 49]. These findings revealed that gut microbiota might drive the colonic mucosa immunological activation via the TLR4 signaling pathway, resulting in neuroinflammation and further neurodegeneration in PD [50]. To further explore the mechanism by which CDG exerts neural protection by replenishing the intestinal microbiota of PD mice, we highlighted the relationship of inflammation between the gut and the brain. Microglia and astrocytes are crucial in maintaining neuronal function and brain homeostasis and are also the primary cells mediating innate immunity in the CNS [51, 52]. When activated, they secrete large quantities of inflammatory chemokines, including TNF- α and IL-1 β [53]. Astrocytes can recognize the TLR mediating inflammatory CNS disease injury [47].

Our study found that microglia and astrocytes were activated in the SNpc of PD mice and were inhibited after CDG administration. Moreover, we labeled TLR4 and TNF- α cells with IF to assess intestinal inflammation. CDG reduced the infiltration of TLR4 and TNF- α cells in PD mice colonic tissue. We also discovered that cytokines (TNF- α , IL-1 β) were raised in PD mice serum, suggesting that proinflammatory factors may penetrate the systemic circulation and cause a systemic inflammatory response. Gut microbial dysbiosis-mediated inflammation leads to the intestine in high permeability to cause "intestinal leakage." Gut barrier integrity is strongly associated with tight junction protein ZO-1 expression in intestinal tissue [24]. ZO-1 expression is lowered in PD mice, and ZO-1 expression is reduced in inflammatory bowel disease (IBD) patients [54, 55]. We examined ZO-1 expression in the mouse colon utilizing IF assay and found that CDG protected the intestinal barrier via restoring tight-junction function. All the data showed that CDG could reconstruct the intestinal microbiota of PD mice to reduce microglia and astrocytes activation, inhibit serum inflammation, and protect the damaged intestinal barrier to play a neuroprotective role.

NF- κ B activating factor TANK-binding kinase 1 (TBK1) is a crucial factor of NF- κ B and has a key part in the inflammatory immune reaction [49, 56]. Inflammatory cytokines stimulate NF- κ B activation in TLR4 signaling through heterodimer RelA (p65) and p50, which translocate to the nucleus and interact with NF- κ B target sites in immune response genes [49]. After TLR4 ligand binding, NF- κ B signaling is activated to discharge proinflammatory cytokines (TNF- α and IL-1 β), which has a crucial function in innate immune defense, neuronal excitotoxicity, and neurodegeneration [57]. Suppressing TLR4-mediated NF- κ B signaling may be a successful approach against PD [58]. FLZ protects rotenone-induced PD mice by ameliorating intestinal dysbiosis and inhibiting TLR4 / MyD88 / NF- κ B signaling pathway in SN and colon [59]. Herein, we further demonstrated the crucial function of activating the TLR4 pathway in the microbe-gut-brain axis involved in PD pathology. Besides reconstructing the dysbiota dysbiosis in PD mice, CDG effectively reduced TLR4, TBK1, NF- κ B, and TNF- α expressions in the PD mice striatum and colon. The molecular mechanisms of CDG in improving dysbiota dysbiosis could be connected to inhibiting TLR4/NF- κ B pathway.

Conclusion

These experiments revealed that CDG regulated dysbiota dysbiosis in MPTP-induced PD mice, reduced neuroinflammation, and induced neuroprotective effects via suppressing TLR4/NF- κ B pathway, offering fresh perspectives for more intensive research. This study has limitations, and in the future, we will include clinical PD patients for validation to further explore the molecular mechanisms of improving PD intestinal microbiosis and exerting neuroprotection.

Declarations

Author contributions

HJC and HZQ designed this study. HZQ and WL have roles in analysis, data interpretation, and manuscript writing. WL and HJC modified the document. HJC, HPF, and WL oversaw the research. All writers reviewed and accepted the final manuscript.

Funding

This research was sponsored by the Youth Science Fund Project of the National Natural Science Fund of China (No.82104965), The National Natural Science Foundation of China (No.81573899), Shanghai Biomedical Science Technology Support Project(20S21901700), and Shanghai Key Laboratory of Health Identification and Assessment (No.21DZ2271000).

Data Availability We declare that the data that support the findings of this study are available from the corresponding author upon reasonable request.

Conflict of interest. The authors declare that they have no conflict of interest.

References

1. Bloem BR, Okun MS, Klein C (2021) Parkinson's disease. *Lancet* 397(10291):2284–2303. [https://doi.org/10.1016/S0140-6736\(21\)00218-X](https://doi.org/10.1016/S0140-6736(21)00218-X)
2. Tolosa E, Garrido A, Scholz SW, Poewe W (2021) Challenges in the diagnosis of Parkinson's disease. *Lancet Neurol* 20(5):385–397. [https://doi.org/10.1016/S1474-4422\(21\)00030-2](https://doi.org/10.1016/S1474-4422(21)00030-2)
3. Jankovic J, Tan EK (2020) Parkinson's disease: etiopathogenesis and treatment. *J Neurol Neurosurg Psychiatry* 91(8):795–808. <https://doi.org/10.1136/jnnp-2019-322338>
4. Travaglini RA, Browning KN, Camilleri M (2020) Parkinson disease and the gut: new insights into pathogenesis and clinical relevance. *Nat Rev Gastroenterol Hepatol* 17(11):673–685. <https://doi.org/10.1038/s41575-020-0339-z>
5. Gazerani P (2019) Probiotics for Parkinson's Disease. *Int J Mol Sci* 20(17):4121. <https://doi.org/10.3390/ijms20174121>
6. Berg D, Postuma RB, Adler CH, Bloem BR, Chan P, Dubois B, Gasser T, Goetz CG, Halliday G, Joseph L, Lang AE, Liepelt-Scarfone I, Litvan I, Marek K, Obeso J, Oertel W, Olanow CW, Poewe W, Stern M, Deuschl G (2015) MDS research criteria for prodromal Parkinson's disease. *Mov Disord* 30(12):1600–1611. <https://doi.org/10.1002/mds.26431>
7. Fasano A, Visanji NP, Liu LW, Lang AE, Pfeiffer RF (2015) Gastrointestinal dysfunction in Parkinson's disease. *Lancet Neurol* 14(6):625–639. [https://doi.org/10.1016/S1474-4422\(15\)00007-1](https://doi.org/10.1016/S1474-4422(15)00007-1)
8. Klann EM, Dissanayake U, Gurralla A, Farrer M, Shukla AW, Ramirez-Zamora A, Mai V, Vedam-Mai V (2022) The Gut-Brain Axis and Its Relation to Parkinson's Disease: A Review. *Front Aging Neurosci* 13:782082. <https://doi.org/10.3389/fnagi.2021.782082>
9. Chen Y, Xu J, Chen Y (2021) Regulation of Neurotransmitters by the Gut Microbiota and Effects on Cognition in Neurological Disorders. *Nutrients* 13(6):2099. <https://doi.org/10.3390/nu13062099>
10. Zhu S, Jiang Y, Xu K, Cui M, Ye W, Zhao G, Jin L, Chen X (2020) The progress of gut microbiome research related to brain disorders. *J Neuroinflammation* 17(1):25. <https://doi.org/10.1186/s12974-020-1705-z>
11. Caputi V, Giron MC (2018) Microbiome-Gut-Brain Axis and Toll-Like Receptors in Parkinson's Disease. *Int J Mol Sci* 19(6):1689. <https://doi.org/10.3390/ijms19061689>
12. West AP, Koblansky AA, Ghosh S (2006) Recognition and signaling by toll-like receptors. *Annu Rev Cell Dev Biol* 22:409–437. <https://doi.org/10.1146/annurev.cellbio.21.122303.115827>
13. Santos SF, de Oliveira HL, Yamada ES, Neves BC, Pereira A Jr (2019) The Gut and Parkinson's Disease-A Bidirectional Pathway. *Front Neurol* 10:574. <https://doi.org/10.3389/fneur.2019.00574>

14. Perez-Pardo P, Kliet T, Dodiya HB, Broersen LM, Garssen J, Keshavarzian A, Kraneveld AD (2017) The gut-brain axis in Parkinson's disease: Possibilities for food-based therapies. *Eur J Pharmacol* 817:86–95. <https://doi.org/10.1016/j.ejphar.2017.05.042>
15. Keshavarzian A, Green SJ, Engen PA, Voigt RM, Naqib A, Forsyth CB, Mutlu E, Shannon KM (2015) Colonic bacterial composition in Parkinson's disease. *Mov Disord* 30(10):1351–1360. <https://doi.org/10.1002/mds.26307>
16. Kuai XY, Yao XH, Xu LJ, Zhou YQ, Zhang LP, Liu Y, Pei SF, Zhou CL (2021) Evaluation of fecal microbiota transplantation in Parkinson's disease patients with constipation. *Microb Cell Fact* 20(1):98. <https://doi.org/10.1186/s12934-021-01589-0>
17. Wang L, Yang YF, Chen L, He ZQ, Bi DY, Zhang L, Xu YW, He JC (2021) Compound Dihuang Granule Inhibits Nigrostriatal Pathway Apoptosis in Parkinson's Disease by Suppressing the JNK/AP-1 Pathway. *Front Pharmacol* 12:621359. <https://doi.org/10.3389/fphar.2021.621359>
18. Zhang JY, Wang L, He JC (2021) A study on the effect of Compound Dihuang Granules in treating the symptoms of the gastrointestinal motility disorder in Parkinson's disease. *J Changchun Univ Chin Med* 37(05):1009–1012. https://kns.cnki.net/kcms/detail/detail.aspx?dbcode=CJFD&dbname=CJFDLAST2021&filename=CZXX202105018&uniplatform=NZKPT&v=WUVx9eTcL5cnwr3fKsh7_2FoERWUE3SgWy6ZhsFEc8L4PDQ4vnxFr5Gz1bpYAhv
19. Bi DY, Wang L, He Zq, Yang YF, He JC (2021) Effects of compound Rehmannia Granule on microglia activation and neurobehavior in Parkinson's Disease model rats. *Acta Lab Anim Sci Sin* 29(06):749–757. https://kns.cnki.net/kcms/detail/detail.aspx?dbcode=CJFD&dbname=CJFDLAST2022&filename=ZGSD202106006&uniplatform=NZKPT&v=FzvRFRbezWGoJe0xgF2VUD1sc0ANrliXFeh41_b8UA3lrEHqMo_IKWaY8Q4qBXcO
20. Zhang R, Zhu X, Bai H, Ning K (2019) Network Pharmacology Databases for Traditional Chinese Medicine: Review and Assessment. *Front Pharmacol* 10:123. <https://doi.org/10.3389/fphar.2019.00123>
21. Nielsen NJ, Andersson AF, Laudon H, Lindström ES, Kritzbeg ES (2016) Experimental insights into the importance of aquatic bacterial community composition to the degradation of dissolved organic matter. *ISME J* 10(3):533–545. <https://doi.org/10.1038/ismej.2015.131>
22. Cheng J, Liao Y, Dong Y, Hu H, Yang N, Kong X, Li S, Li X, Guo J, Qin L, Yu J, Ma C, Li J, Li M, Tang B, Yuan Z (2020) Microglial autophagy defect causes parkinson disease-like symptoms by accelerating inflammasome activation in mice. *Autophagy* 16(12):2193–2205. <https://doi.org/10.1080/15548627.2020.1719723>
23. Lee Y, Lee S, Chang SC, Lee J (2019) Significant roles of neuroinflammation in Parkinson's disease: therapeutic targets for PD prevention. *Arch Pharm Res* 42(5):416–425. <https://doi.org/10.1007/s12272-019-01133-0>
24. Dodiya HB, Forsyth CB, Voigt RM, Engen PA, Patel J, Shaikh M, Green SJ, Naqib A, Roy A, Kordower JH, Pahan K, Shannon KM, Keshavarzian A (2020) Chronic stress-induced gut dysfunction exacerbates Parkinson's disease phenotype and pathology in a rotenone-induced mouse model of Parkinson's disease. *Neurobiol Dis* 135:104352. <https://doi.org/10.1016/j.nbd.2018.12.012>
25. Liang Jq, He JC (2019) Effects of Fufang Dihuang Decoction on behavior and monoamine neurotransmitters in corpus striatum of PD mice. *Chin J Tradit Med and Pharm* 34(02):742–745. https://kns.cnki.net/kcms/detail/detail.aspx?dbcode=CJFD&dbname=CJFDLAST2019&filename=BXY201902086&uniplatform=NZKPT&v=AZzwea4pqFXQdgr26QbcNptFWOhNesQMk_wtFfWx3XxKflyBoZuoDC
26. Tan AH, Lim SY, Lang AE (2022) The microbiome-gut-brain axis in Parkinson disease—from basic research to the clinic. *Nat Rev Neurol* 18(8):476–495. <https://doi.org/10.1038/s41582-022-00681-2>
27. Cryan JF, O'Riordan KJ, Cowan CSM, Sandhu KV, Bastiaanssen TFS, Boehme M, Codagnone MG, Cussotto S, Fulling C, Golubeva AV, Guzzetta KE, Jaggar M, Long-Smith CM, Lyte JM, Martin JA, Molinero-Perez A, Moloney G, Morelli E, Morillas E, O'Connor R, Cruz-Pereira JS, Peterson VL, Rea K, Ritz NL, Sherwin E, Spichak S, Teichman EM, van de Wouw M, Ventura-Silva AP, Wallace-Fitzsimons SE, Hyland N, Clarke G, Dinan TG (2019) The Microbiota-Gut-Brain Axis. *Physiol Rev* 99(4):1877–2013. <https://doi.org/10.1152/physrev.00018.2018>
28. Kin K, Yasuhara T, Kameda M, Date I (2019) Animal Models for Parkinson's Disease Research: Trends in the 2000s. *Int J Mol Sci* 20(21):5402. <https://doi.org/10.3390/ijms20215402>
29. Javitch JA, D'Amato RJ, Strittmatter SM, Snyder SH (1985) Parkinsonism-inducing neurotoxin, N-methyl-4-phenyl-1,2,3,6-tetrahydropyridine: uptake of the metabolite N-methyl-4-phenylpyridine by dopamine neurons explains selective toxicity. *Proc Natl Acad Sci U S A* 82(7):2173–2177. <https://doi.org/10.1073/pnas.82.7.2173>
30. Bezaud E, Gross CE, Fournier MC, Dovero S, Bloch B, Jaber M (1999) Absence of MPTP-induced neuronal death in mice lacking the dopamine transporter. *Exp Neurol* 155(2):268–273. <https://doi.org/10.1006/exnr.1998.6995>
31. Martí Y, Matthaeus F, Lau T, Schloss P (2017) Methyl-4-phenylpyridinium (MPP+) differentially affects monoamine release and re-uptake in murine embryonic stem cell-derived dopaminergic and serotonergic neurons. *Mol Cell Neurosci* 83:37–45. <https://doi.org/10.1016/j.mcn.2017.06.009>
32. Ayala A, Muñoz MF, Argüelles S (2014) Lipid peroxidation: production, metabolism, and signaling mechanisms of malondialdehyde and 4-hydroxy-2-nonenal. *Oxid Med Cell Longev*. 2014:360438. <https://doi.org/10.1155/2014/360438>
33. Wei Z, Li X, Li X, Liu Q, Cheng Y (2018) Oxidative Stress in Parkinson's Disease: A Systematic Review and Meta-Analysis. *Front Mol Neurosci* 11:236. <https://doi.org/10.3389/fnmol.2018.00236>
34. Sun MF, Zhu YL, Zhou ZL, Jia XB, Xu YD, Yang Q, Cui C, Shen YQ (2018) Neuroprotective effects of fecal microbiota transplantation on MPTP-induced Parkinson's disease mice: Gut microbiota, glial reaction and TLR4/TNF- α signaling pathway. *Brain Behav Immun* 70:48–60. <https://doi.org/10.1016/j.bbi.2018.02.005>
35. Jang JH, Yeom MJ, Ahn S, Oh JY, Ji S, Kim TH, Park HJ (2020) Acupuncture inhibits neuroinflammation and gut microbial dysbiosis in a mouse model of Parkinson's disease. *Brain Behav Immun* 89:641–655. <https://doi.org/10.1016/j.bbi.2020.08.015>
36. Zhou ZL, Jia XB, Sun MF, Zhu YL, Qiao CM, Zhang BP, Zhao LP, Yang Q, Cui C, Chen X, Shen YQ (2019) Neuroprotection of Fasting Mimicking Diet on MPTP-Induced Parkinson's Disease Mice via Gut Microbiota and Metabolites. *Neurotherapeutics* 16(3):741–760. <https://doi.org/10.1007/s13311-019->

37. Hopfner F, Künstner A, Müller SH, Künzel S, Zeuner KE, Margraf NG, Deuschl G, Baines JF, Kuhlenbäumer G (2017) Gut microbiota in Parkinson disease in a northern German cohort. *Brain Res* 1667:41–45. <https://doi.org/10.1016/j.brainres.2017.04.019>
38. Keshavarzian A, Green SJ, Engen PA, Voigt RM, Naqib A, Forsyth CB, Mutlu E, Shannon KM (2015) Colonic bacterial composition in Parkinson's disease. *Mov Disord* 30(10):1351–1360. <https://doi.org/10.1002/mds.26307>
39. Li C, Cui L, Yang Y, Miao J, Zhao X, Zhang J, Cui G, Zhang Y (2019) Gut Microbiota Differs Between Parkinson's Disease Patients and Healthy Controls in Northeast China. *Front Mol Neurosci* 12:171 Published 2019 Jul 11. <https://doi.org/10.3389/fnmol.2019.00171>
40. Baldini F, Hertel J, Sandt E, Thinnies CC, Neuberger-Castillo L, Pavelka L, Betsou F, Krüger R, Thiele I (2020) Parkinson's disease-associated alterations of the gut microbiome predict disease-relevant changes in metabolic functions. *BMC Biol* 18(1):62. <https://doi.org/10.1186/s12915-020-00775-7>
41. Murros KE, Huynh VA, Takala TM, Saris PEJ (2021) Desulfotribium Bacteria Are Associated With Parkinson's Disease. *Front Cell Infect Microbiol* 11:652617. <https://doi.org/10.3389/fcimb.2021.652617>
42. Ferri V, Cassani E, Bonvegna S, Ferrarese C, Zecchinelli AL, Barichella M, Pezzoli G (2021) Does Gut Microbiota Influence the Course of Parkinson's Disease? A 3-Year Prospective Exploratory Study in de novo Patients. *J Parkinsons Dis* 11(1):159–170. <https://doi.org/10.3233/JPD-202297>
43. Li N, Wang X, Sun C, Wu X, Lu M, Si Y, Ye X, Wang T, Yu X, Zhao X, Wei N, Wang X (2019) Change of intestinal microbiota in cerebral ischemic stroke patients. *BMC Microbiol* 19(1):191. <https://doi.org/10.1186/s12866-019-1552-1>
44. Wang CS, Li WB, Wang HY, Ma YM, Zhao XH, Yang H, Qian JM, Li JN (2018) VSL#3 can prevent ulcerative colitis-associated carcinogenesis in mice. *World J Gastroenterol* 24(37):4254–4262. doi:10.3748/wjg.v24.i37.4254
45. Wu M, Yang S, Wang S, Cao Y, Zhao R, Li X, Xing Y, Liu L (2020) Effect of Berberine on Atherosclerosis and Gut Microbiota Modulation and Their Correlation in High-Fat Diet-Fed ApoE^{-/-} Mice. *Front Pharmacol* 11:223. <https://doi.org/10.3389/fphar.2020.00223>
46. Wang Q, Luo Y, Ray Chaudhuri K, Reynolds R, Tan EK, Pettersson S (2021) The role of gut dysbiosis in Parkinson's disease: mechanistic insights and therapeutic options. *Brain* 144(9):2571–2593. <https://doi.org/10.1093/brain/awab156>
47. Xia P, Wu Y, Lian S, Yan L, Meng X, Duan Q, Zhu G (2021) Research progress on Toll-like receptor signal transduction and its roles in antimicrobial immune responses. *Appl Microbiol Biotechnol* 105(13):5341–5355. <https://doi.org/10.1007/s00253-021-11406-8>
48. Rodríguez-Gómez JA, Kavanagh E, Engskog-Vlachos P, Engskog MKR, Herrera AJ, Espinosa-Oliva AM, Joseph B, Hajji N, Venero JL, Burguillos MA (2020) Microglia: Agents of the CNS Pro-Inflammatory Response. *Cells* 9(7):1717. <https://doi.org/10.3390/cells9071717>
49. Fitzgerald KA, Kagan JC (2020) Toll-like Receptors and the Control of Immunity. *Cell* 180(6):1044–1066. <https://doi.org/10.1016/j.cell.2020.02.041>
50. Heidari A, Yazdanpanah N, Rezaei N (2022) The role of Toll-like receptors and neuroinflammation in Parkinson's disease. *J Neuroinflammation* 19(1):135. <https://doi.org/10.1186/s12974-022-02496-w>
51. David FS, Scholz C, Shihui F, Lum J, Amoyo AA, Larbi A, Poidinger M, Buttgerit A, Lledo PM, Greter M, Chan JKY, Amit I, Beyer M, Schultze JL, Schlitzer A, Pettersson S, Ginhoux F, Garel S (2018) Microbiome Influences Prenatal and Adult Microglia in a Sex-Specific Manner. *Cell* 172(3):500–516. <https://doi.org/10.1016/j.cell.2017.11.042>
52. Li L, Acioglu C, Heary RF, Elkabes S (2021) Role of astroglial toll-like receptors (TLRs) in central nervous system infections, injury and neurodegenerative diseases. *Brain Behav Immun* 91:740–755. <https://doi.org/10.1016/j.bbi.2020.10.007>
53. Lehnardt S (2010) Innate immunity and neuroinflammation in the CNS: the role of microglia in Toll-like receptor-mediated neuronal injury. *Glia* 2010 58(3):253–263. <https://doi.org/10.1002/glia.20928>
54. Zhao Z, Li F, Ning J, Peng R, Shang J, Liu H, Shang M, Bao XQ, Zhang D (2021) Novel compound FLZ alleviates rotenone-induced PD mouse model by suppressing TLR4/MyD88/NF- κ B pathway through microbiota-gut-brain axis. *Acta Pharm Sin B* 11(9):2859–2879. <https://doi.org/10.1016/j.apsb.2021.03.020>
55. Kuo WT, Zuo L, Odenwald MA, Madha S, Singh G, Gurniak CB, Abraham C, Turner JR (2021) The Tight Junction Protein ZO-1 Is Dispensable for Barrier Function but Critical for Effective Mucosal Repair. *Gastroenterology* 161(6):1924–1939. <https://doi.org/10.1053/j.gastro.2021.08.047>
56. Satoh T, Akira S (2016) Toll-Like Receptor Signaling and Its Inducible Proteins. *Microbiol Spectr* 4(6):10. <https://doi.org/10.1128/microbiolspec.MCHD-0040-2016>
57. Leitner GR, Wenzel TJ, Marshall N, Gates EJ, Klegeris A (2019) Targeting toll-like receptor 4 to modulate neuroinflammation in central nervous system disorders. *Expert Opin Ther Targets* 23(10):865–882. <https://doi.org/10.1080/14728222.2019.1676416>
58. Chen H, Zhong J, Li J, Zeng Z, Yu Q, Yan C (2022) PTP70-2, a novel polysaccharide from *Polygala tenuifolia*, prevents neuroinflammation and protects neurons by suppressing the TLR4-mediated MyD88/NF- κ B signaling pathway. *Int J Biol Macromol* 194:546–555. <https://doi.org/10.1016/j.ijbiomac.2021.11.097>
59. Zhao Z, Ning J, Bao XQ, Shang M, Ma J, Li G, Zhang D (2021) Fecal microbiota transplantation protects rotenone-induced Parkinson's disease mice via suppressing inflammation mediated by the lipopolysaccharide-TLR4 signaling pathway through the microbiota-gut-brain axis. *Microbiome* 9(1):226. <https://doi.org/10.1186/s40168-021-01107-9>

Table 1

Table 1 is available in the Supplementary Files section.

Figures

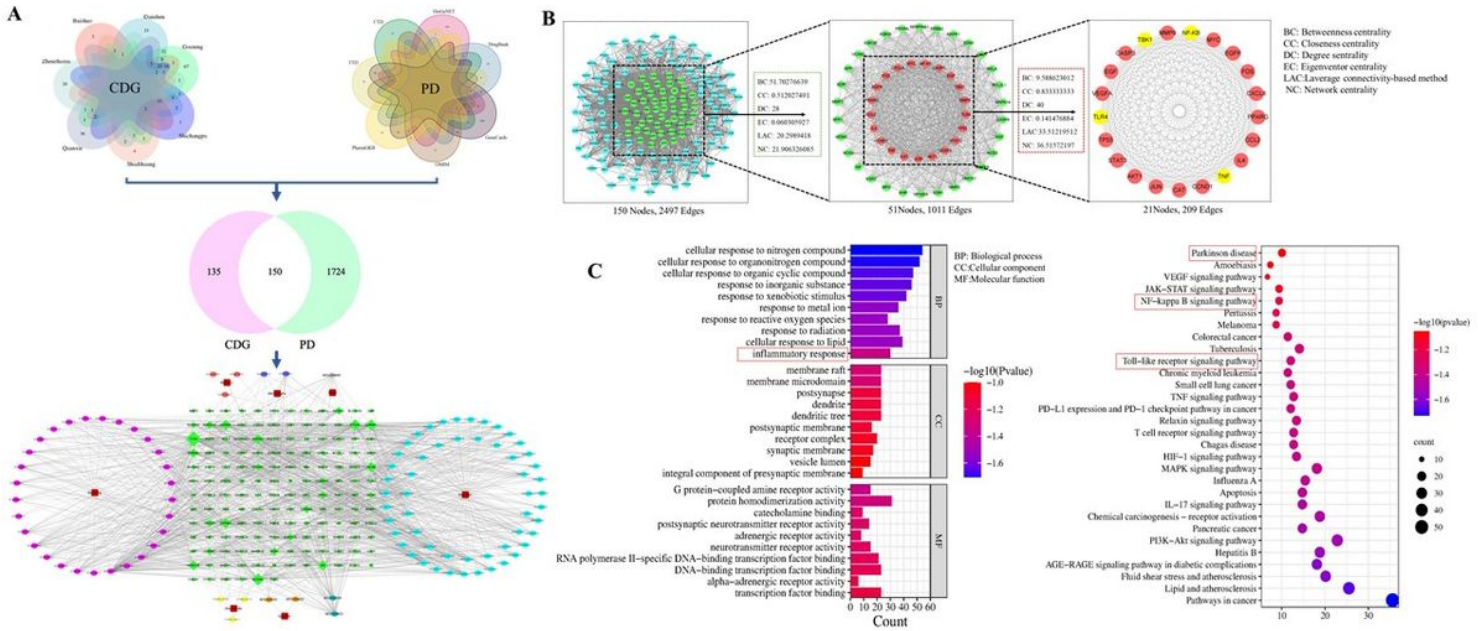


Fig. 1. Network pharmacology and molecular docking analyses of CDG treatment in PD. (A) Developing a CDG ingredient-target network, the red squares indicate herbs; the green diamond nodes represent targets; the colored circular nodes indicate ingredients from different herbs; the big size circular is closer related to the centrality; (B) composition-target network of CDG; 21 important targets were finally screened out; (C) enrichment results for GO functions and KEGG pathways for CDG versus PD; the top-30 terms in every GO category and significant changes of top-30 pathways were identified according to the P -value < 0.05 .

Figure 1

See image above for figure legend

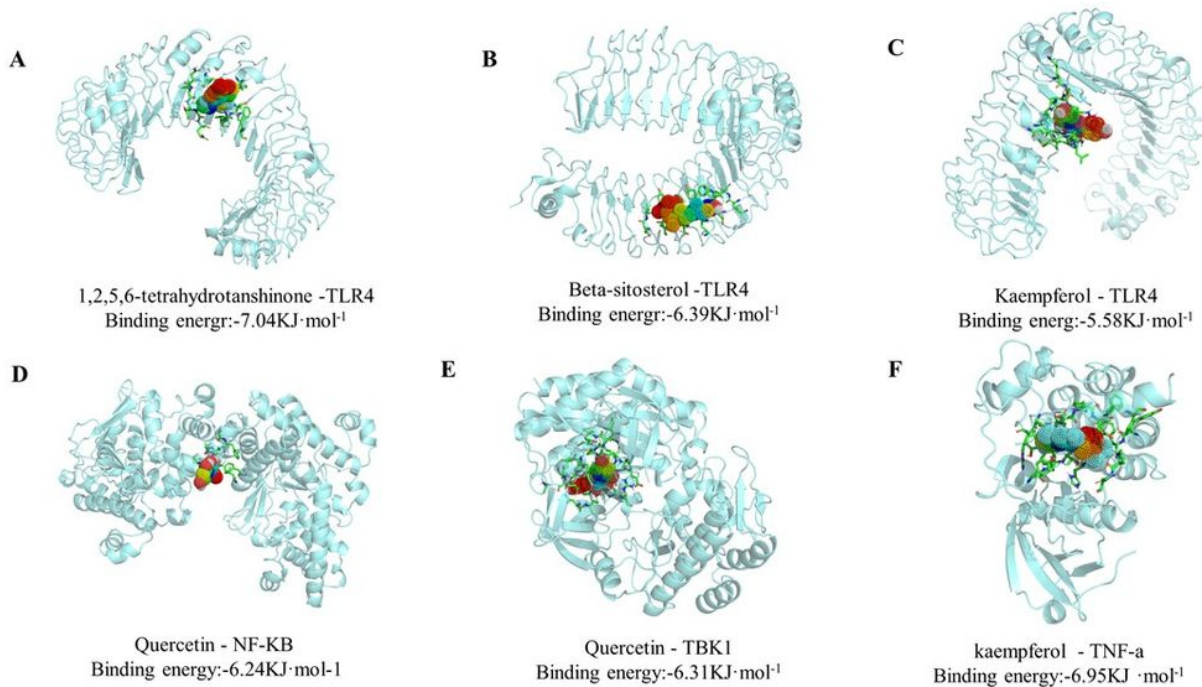


Fig. 2. Docking of active ingredients with TLR4/NF-κB. (A) 1,2,5,6-tetrahydroanthinone -TLR4; (B) Beta-sitosterol-TLR4; (C) Kaempferol-TLR4; (D) Quercetin-NF-KB; (E) Quercetin-TBK1; (F) kaempferol - TNF-a.

Figure 2

See image above for figure legend

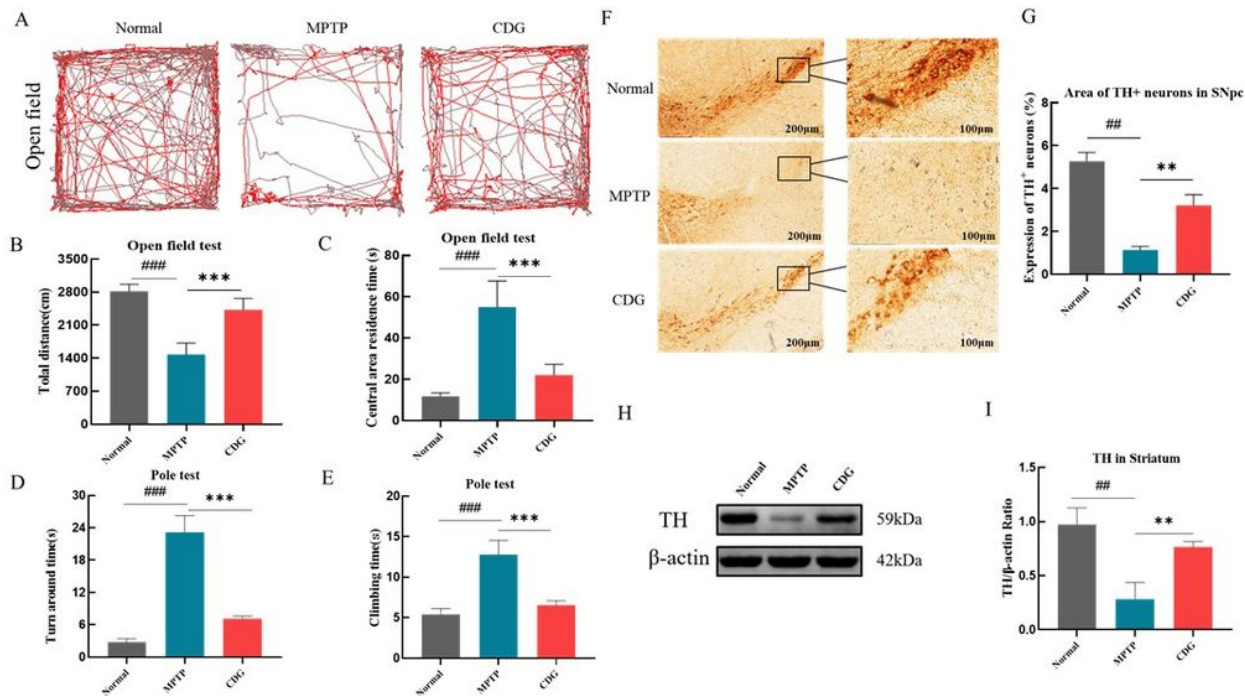


Fig.3. CDG treatment increased dopaminergic neuronal and improved motor functions in MPTP-induced PD mice. (A) Mice autonomous activity trajectories were recorded during the Open field exam; (B) total motor distance of the mice in five minutes; (C) stay time in the central area; (D) mice turnaround time during the Pole exam; (E) mice climbing time during the Pole exam; (F) IHC staining of TH in SN; the scale bar is 200 μm; 100 μm; (G) the outcome of TH WB density analysis in Striatum; (H) TH expression in the Striatum with WB; (I) TH⁺ neuron cells count in SN; one-way analysis of variance was employed to evaluate the data; n = 8 for the behavioral test; n = 3 for WB and IHC; findings are shown as mean ± SD, vs. Normal; ###*P* < 0.001; vs. MPTP; ****P* < 0.001.

Figure 3

See image above for figure legend

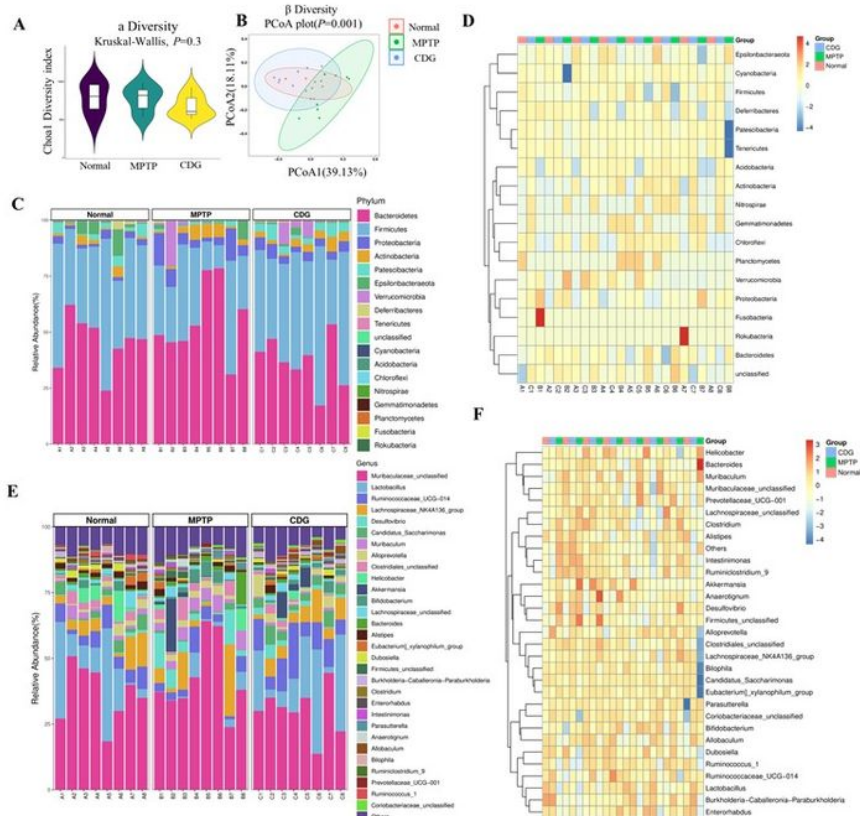


Fig.4. CDG treatment improved the dysbiosis of gut microbes of MPTP-induced PD mice. (A) Chao1 analysis of the alpha diversity of gut microbiota; (B) beta diversity according to a weighted UniFrac ANOSIM study in several color-coded groups; (C) relative predominance of gut microbiota at the Phylum level in each group; (D) Heatmap analysis of relative predominance of gut microbiota at the Phylum level for various groups; (E) relative predominance of gut microbiota at the Genus level for each group; (F) Heatmap analysis of relative predominance of gut microbiota at the Genus level in various groups; the data were analyzed with Kruskal-Wallis; n = 8.

Figure 4

See image above for figure legend

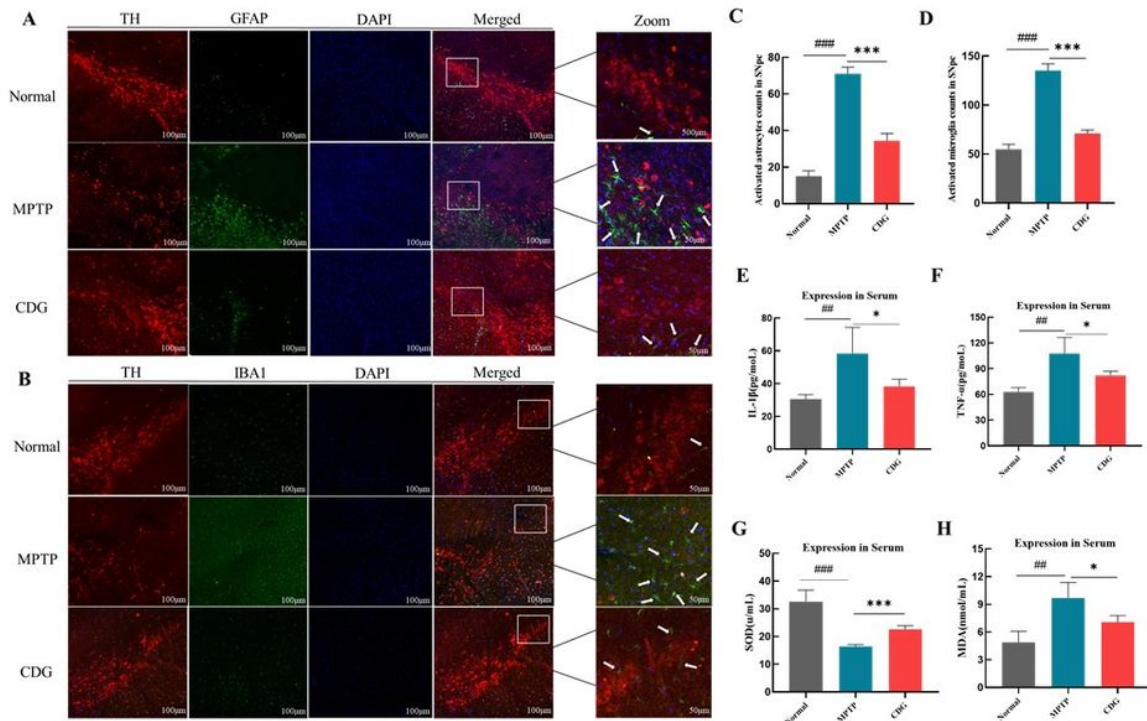


Fig.5. In MPTP-induced PD mice, CDG treatment suppressed the PD-associated inflammation and oxidative stress. (A) IF staining for TH (Red) and GFAP (Green) in the SNpc; (B) IF staining for TH (Red) and IBA1 (Green) in the SNpc; (C-D) the proportion of activated astrocytes and microglia in the SNpc; (E-F) IL-1 β ; TNF- α serum expressions; (G-H) SOD; MDA serum expressions; white arrows represent the positive cells in SNpc; scale bar is 100 μ m; 50 μ m; findings are assessed with a One-way ANOVA; n = 3 for IF; n = 4 for ELISA; findings are presented as mean \pm SD, VS Normal; $^{##}P < 0.01$; $^{###}P < 0.001$; vs. MPTP; $^{*}P < 0.05$; $^{***}P < 0.001$.

Figure 5

See image above for figure legend

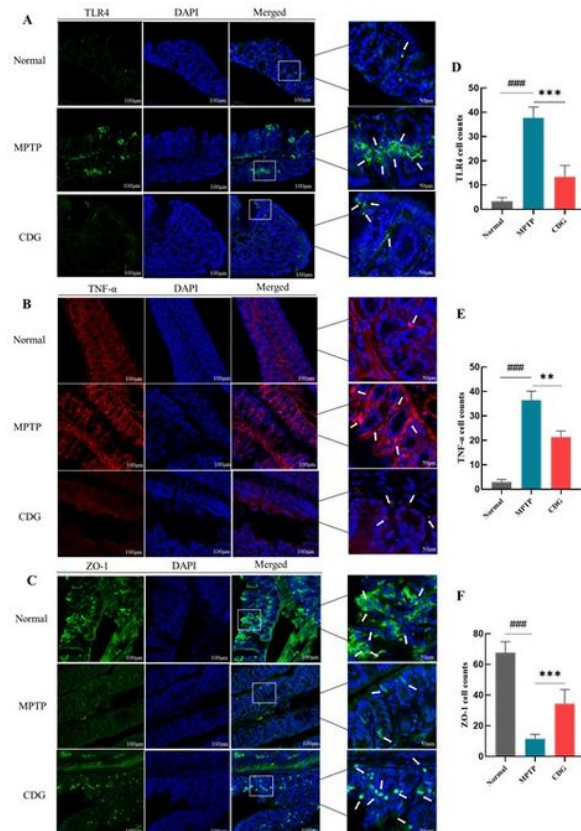


Fig. 6. CDG treatment suppressed the inflammatory proteins in the colon and protected the intestinal barrier in MPTP-induced PD mice. (A-C) IF staining for TLR4 (Green); TNF- α (Red); and ZO-1 (Green) in the colon; (D-F) the numbers of TLR4; TNF- α ; and ZO-1 cells in the colon; white arrows present the positive cells in the colon; the scale bar was 100 μ m; 50 μ m; the data are assessed utilizing a One-way ANOVA; n = 3 for IF; findings are demonstrated as mean \pm SD; vs. Normal, $^{###}P < 0.001$; vs. MPTP, $^{**}P < 0.01$, $^{***}P < 0.001$.

Figure 6

See image above for figure legend

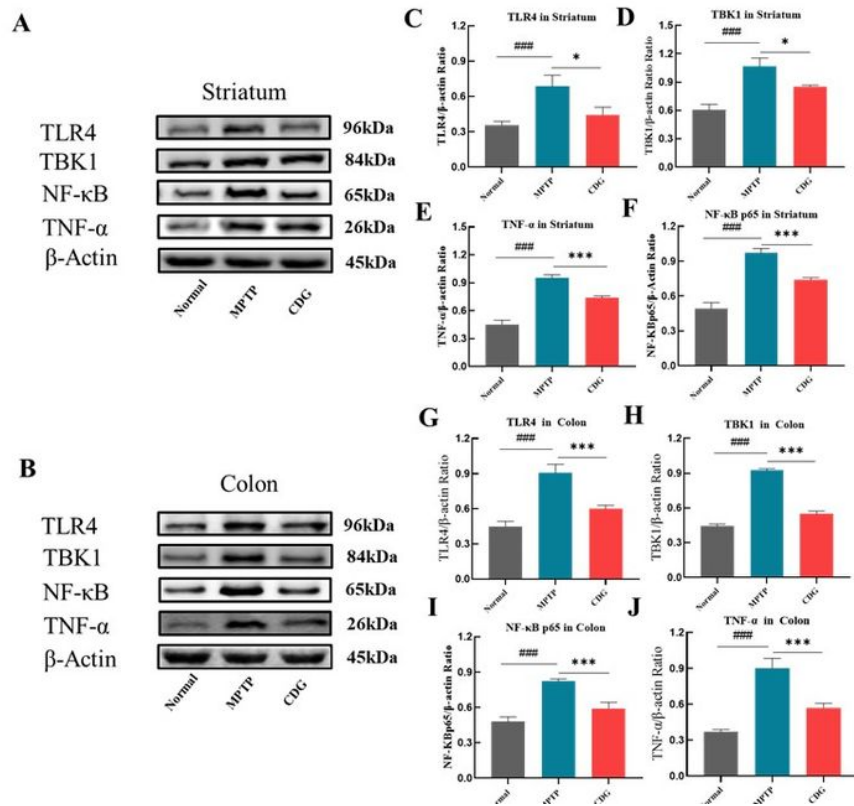


Fig. 7. CDG treatment alleviated intestinal inflammation and neuroinflammation via blocking TLR4/NF-κB pathway in MPTP-induced PD mice. (A) Representative WB bands of TLR4; TBK1; NF-κB; and TNF-α in the striatum; (C-F) the density analysis results of TLR4; TBK1; NF-κB; TNF-α in the striatum; (B) representative WB bands of TLR4; TBK1; NF-κB; and TNF-α in the colon; (G-J) the density analysis results of TLR4; TBK1; NF-κB; TNF-α in the colon; findings are assessed with a one-way ANOVA, n = 3 for WB; findings are reported as mean ± SD, VS Normal; ####P < 0.001; vs. MPTP; *P < 0.05; ***P < 0.001.

Figure 7

See image above for figure legend

Supplementary Files

This is a list of supplementary files associated with this preprint. Click to download.

- [table1.jpg](#)
- [SupplementaryFile.zip](#)